

Investigation of Geostrophic and Ekman Surface Current Using Satellite Altimetry Observations and Surface Wind in Persian Gulf and Oman Sea

Farzaneh, S.^{1*}, Parvazi, K.² and Noroozi, T.³

1. Assistant Professor, Department of Surveying and Geomatics Engineering, Faculty of Engineering, University of Tehran, Iran

2. Ph.D. Student, Department of Surveying and Geomatics Engineering, Faculty of Engineering, University of Tehran, Iran

3. M.Sc. Student, Department of Surveying Engineering, faculty of Engineering, University of Zanjan, Zanjan, Iran

(Received: 11 Nov 2017, Accepted: 6 Feb 2018)

Abstract

The rise of satellite altimetry is a revolution in the ocean sciences. Due to its global coverage and its high resolution, altimetry classically outperforms in situ water level measurement. Ekman and geostrophic currents are large parts of the ocean's current, playing a vital role in global climate variations. According to the classic oceanography, Ekman and geostrophic currents can be calculated through the pressure gradient force as well as the friction force assuming that the water's density is constant. Investigation of Ekman and geostrophic currents existence along with the determination of their velocities can profoundly affect the various events of oceanography and different interactive processes between the atmosphere and the ocean. Additionally, the measurement of sea currents can be useful in determination of contamination transport, seawater exchange, fisheries, oil transfer, immigration of aquatic animals and several marine activities (e.g. military, telecommunication, fishing and research activities) and also has different effects on the regional climate. In the current study, local and climatic conditions, Ekman and geostrophic currents and their velocities have been investigated based on the solution of Ekman and geostrophic equilibrium equations in the region of the Persian Gulf and the Oman Sea. To this end, using data of Saral and Jason-2 altimetry satellites and surface wind data measured by ASCAT satellite, velocities values of v and u as well as the value and the direction of Ekman and geostrophic currents were extracted in forms of monthly data. The results were compared with obtained measurements by AVISO and NOAA for the region of the Persian Gulf and the Oman Sea, and based on the obtained results of this study, the difference in the value of these currents is about 1 cm/s.

Keywords: Ekman current; Geostrophic current; Surface wind; Wind stress, Satellite altimetry.

1. Introduction

The Persian Gulf and the Oman Sea benefit from a special location due to their specific climatic features. The Oman Sea is in a direct connection to the Arabian Sea and the Indian Ocean and is known as a deep sea. On the other hand, the Persian Gulf is a semi-closed and shallow marine environment connected to the Oman Sea by the Strait of Hormuz and is known as one of the most important waterways in the world, from economic and political viewpoints. Study of currents of the Persian Gulf and the Oman Sea is so vital because of their effects on the regional climate, the environment, fisheries, shape change of coastal areas, maritime transportations as well as affecting oil and non-oil pollution movements. Today, by the development and expansion of satellite observations, the trend of sea surface currents

can be extracted using physical and mathematical methods (Fleet and Weiss, 2005; Bowditch, 2012).

Ocean surface currents are mainly due to winds and their effects are dominant in upper layers, while the density-induced currents mainly affect deeper parts of the ocean (Aken, 2007). According to the movement direction of upper layers, the direction of sea surface currents can be realized, which are beneficial for determining climate changes as a condition in ocean's boundaries for the atmospheric models (Reynolds and Smith, 1994). Two important factors standing out the most are the wind force and the water density difference giving rise to the creation of sea surface currents (Dawe and Thompson, 2006), (Zonn et al., 2010). Moreover, other factors can also lead to the

*Corresponding author:

farzaneh@ut.ac.ir

changes in the sea surface currents including water's depth, seabed topography, land dimensions and positions (Bowditch, 2012). In this regard, the knowledge of Ekman and geostrophic surface current changes is essential for realizing oceans dynamics and mechanism as well as mass and heat transfer. By now, several studies have been performed based on the values of altimetry data and the effect of the wind on the water surface movement in the field of ocean currents. Scharffenberg and Stammer (2010) presented the obtained results of the consecutive missions of Jason-TOPEX/Poseidon satellite for local structure of current annual changes in a global scale. Nansen (1898) presented the theory of the wind stress-induced current, which discussed the fact that ice mountains in the Polar Regions in the northern hemisphere did not move in the wind direction, but they deviate. The value of the movement deviation was reported by Nansen as 20-40° to the right of wind direction. Sverdrup (1947) indicated that the current in long distances at top of the ocean is directly connected with the wind stress. Stommel (1948) showed that the current in the oceanic cycle is asymmetric due to the fact that the Coriolis force changes with the latitude. Munk (1950) calculated the current at upper layers of the Pacific Ocean by adding the vortex viscosity.

The aim of this work is to calculate geostrophic surface currents by the balance between the Coriolis force and the horizontal pressure gradient through observations of Topex satellite altimetry as well as measuring Ekman surface currents by the equilibrium between the Coriolis force and the friction force using calculated surface wind data. To this end, the distance of the satellite from the sea surface is calculated from observations of Saral and Jason-2 altimetry satellites and thereby the gridded data of sea surface height (SSH) is created. One application of the SSH is the extraction of geostrophic surface currents (Deng et al., 2011). To this end, first, the absolute dynamic topography (ADT) is achieved by the difference between the SSH and the geoid (AVISO, 2012), and finally, the geostrophic surface current is calculated regarding the absolute dynamic topography. In association with the geostrophic surface current, within oceans

and far from the upper and lower parts of Ekman layers, both pressure gradient and Coriolis forces are in equilibrium for usually long distances and for a certain time. This equilibrium is known as the geostrophic equilibrium (Stewart, 2009). In order to explain the water movement induced by the wind drift resulting from the wind stress on the water surface, Ekman theory that is one of the theories used in oceanic circulation study due to the wind drift is also used. Ekman (1905) suggested that under certain conditions (stable conditions), wind uniform stress, Coriolis force and friction force are in equilibrium in the surface layer (Nitta and Yamada, 1989). With the increase of depth in Ekman layer, the current deviation is created due to the Coriolis force. Surface currents that are created due to the wind, deviate 45° toward the right and the left direction of the wind in the northern and southern hemisphere, respectively (Stewart, 2009).

2. Data

In this work, in order to determine the geoid altimetry data (Saral, Jason-2), sea surface height and daily data of satellite wind speed ASCAT as well as the wind speed and its direction, three datasets including geoid data EGM08 (earth gravity model) were utilized. In order to access the geoid, satellite altimetry and surface wind speed data, three websites, namely, "<http://icgem.gfz-potsdam.De/ICGEM/>", "<http://www.aviso.oceanobs.com>" and "<http://oceanwatch.pifsc.noaa.gov>" were used respectively. In the following sections, this aforementioned data will be briefly introduced.

2-1. Geoid

In this study, the presented geoid by ICGEM service in the region of the Persian Gulf and the Oman Sea was used. These data are for an oval WGS84 with the equatorial radius of 6378.1363 km and the compression coefficient of 1/298.257. Considering the EGM08 model and determining 0.5-degree grids in the region of the Persian Gulf and the Oman Sea (latitude of 22-31° North and longitude of 47-65° East), the geoid height data can be extracted. Figure 1 illustrates the obtained geoid in the region of the Persian Gulf and

the Oman Sea for January 2014 using the mentioned model.

2-2. Altimetry Data

The applied altimetry data in this study are corrected SSH data for both Saral and Jason-2 altimetry satellites in an identical time period. Due to the presence of various layers of the atmosphere between the satellite and the sea level, errors are introduced the observations. In fact, corrected data are data in which the effects of the wet troposphere error (Δw), dry troposphere error (Δd), ionosphere error (ΔI), seawater tide error, polar tide error (ΔpT), inverse pressure effect bias (ΔIB), sea state bias, electromagnetic bias (ΔE) and error of center of gravity changes of altimeter antenna (Δc) are applied. At first, SSH can be obtained based on instant sea level (ISL) and some equations (Parvazi et al. 2015, Andersen, 2010, Forman, 1998) observing the altimetry satellite and applying the above-mentioned corrections. The altimetry data used in this study has been processed using the Basic Radar Altimetry Toolbox (BRAT) software. This software is available at: http://earth.esa.int/BRAT/html/data/toolbox_en.html. The data analysis and coding step

in MATLAB software were also carried out.

Regarding the Equation (1), sea surface height can be calculated relative to the reference ellipsoid.

$$SSH(\varphi, \lambda, t) = H_{sat}(\varphi, \lambda, t) - Range(\varphi, \lambda, t) \quad (1)$$

Where H_{sat} is the satellite height from the reference ellipsoid and $Range$ is the satellite height relative to sea level. In order to determine the corrected height of sea level relative to the reference ellipsoid, firstly, the corrected distance between the satellite and sea level should be calculated using the following equation, and then the corrected SSH can be attained through the Equation (3).

$$\text{Corrected Range} = Range + \Delta w + \Delta d + \Delta I + \Delta IB + \Delta c + \Delta pT + \Delta E \quad (2)$$

$$SSH(\lambda, \varphi, t) = H_{sat}(\lambda, \varphi, t) - \text{Corrected Range}(\lambda, \varphi, t) \quad (3)$$

Figure 2 demonstrates the observations measurement method using the altimetry satellites.

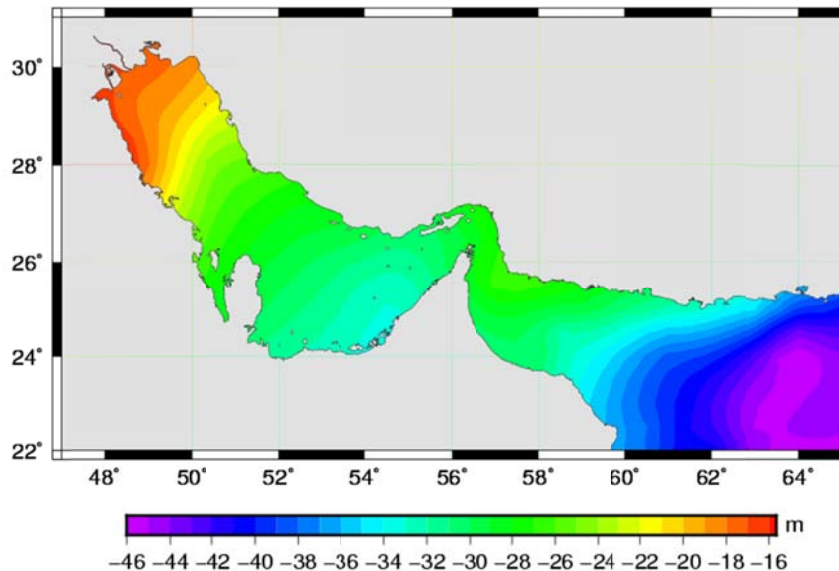


Figure 1. Geoid height EGM2008 model - for January 2014.

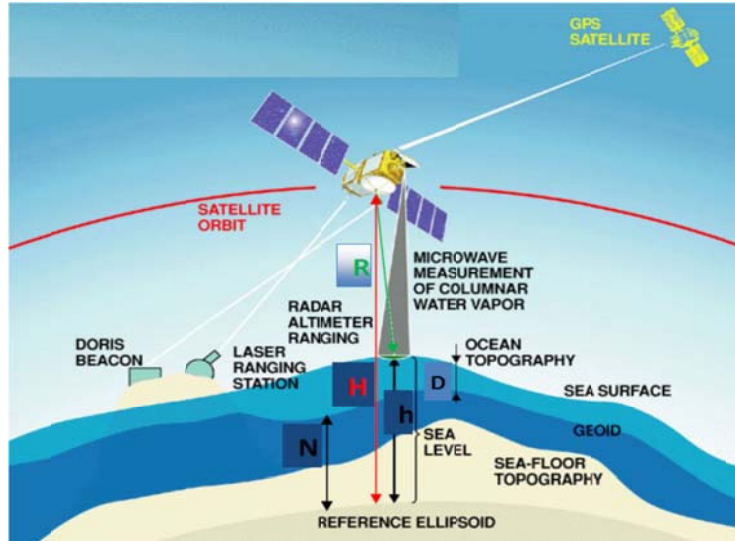


Figure 2. The basis of altimetry satellites measurement (Picot et al. 2003).

Obtained SSH data from these satellites in the region of the Persian Gulf and the Oman Sea in a monthly time period were used in the year 2014. Passages of mentioned satellites for the region of the Persian Gulf and the Oman Sea is shown in Figure 3.

2-3. Surface Wind

The most indispensable factor in the creation of sea surface currents is wind (Bowditch, 2012). Therefore, in order to study surface currents precisely, the effect of wind should be taken into account. This effect is in direct connection with the water's depth. In this

regard, in shallow waters, sea surface currents are frequently in the same direction as the sea surface winds. In this study, remote sensing information of the ASCAT satellite was used to obtain surface wind data. ASCAT data are presented daily and with the time average of three days, weekly and monthly. These data are designed based on a grid with the spatial density of 0.5 degrees. Surface wind data of this satellite is for a height of 10 meters above the sea level. The value and the direction of the surface wind speed for January 2014 are presented in Figure 4.

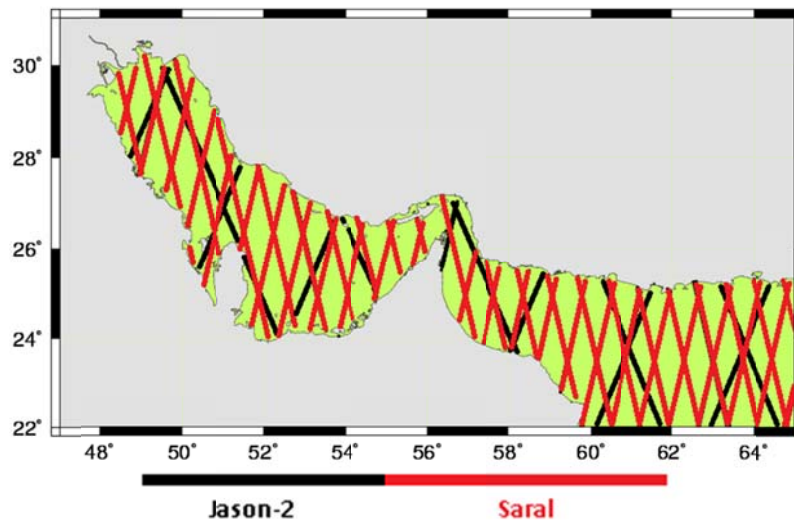


Figure 3. Passages of mentioned satellites Jason-2 (color black) and Saral (color red) for the region of the Persian Gulf and the Oman Sea.

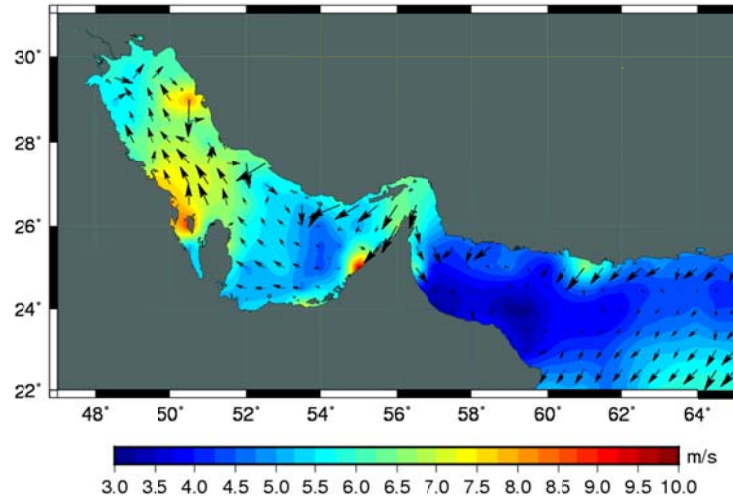


Figure 4. The value and direction of the surface wind speed (m/s) in January 2014.

3. Research Methodology

In this work, Ekman and geostrophic equations were used in order to calculate Ekman and geostrophic currents as well as the surface wind stress. First, the absolute dynamic topography was estimated using geoid data and satellite altimetry, and then the surface wind stress was extracted using surface wind data. Therefore, in the first step, the direction and velocity of the geostrophic current were calculated using the absolute dynamic topography and geostrophic equations, and then the direction, and the velocity of the Ekman current was calculated using the surface wind stress and Ekman equations.

3-1. Absolute Dynamic Topography (ADT) and Surface Geostrophic Current (SGC)

The surface geostrophic current is calculated considering the absolute dynamic topography. The following equation can be used to calculate the absolute dynamic topography (Shum and Braun, 2004):

$$ADT = SSH - N \quad (4)$$

where N is the geoid height and SSH is the sea surface height.

The velocity of the surface geostrophic current, $U_s = u_s + iv_s$, in zonal or eastern components terms u_s , and meridional or northern component v_s , along towards the east direction (x) and north direction (y); directly conforms to geostrophic equations. According to the following

equation and by assuming that the water density remains constant, the velocity of the surface geostrophic current for zonal and meridional components can be achieved (Stewart, 2008).

$$\begin{aligned} U_s(t) &= -\frac{1}{\rho f} \frac{\partial p}{\partial y} = -\frac{g}{f} \frac{\partial ADT(t)}{\partial y} \\ V_s(t) &= \frac{1}{\rho f} \frac{\partial p}{\partial x} = \frac{g}{f} \frac{\partial ADT(t)}{\partial x} \end{aligned} \quad (5)$$

Where g is the gravitational acceleration, p is the pressure obtained by using $p = \rho gh$, and h represents the absolute dynamic topography; f is the Coriolis parameter ($f = 2\Omega \sin\phi$; in this equation, Ω is the earth's rotation rate). If $\phi \rightarrow 0$, numerical calculations of Equation (2) would be vague. In order to solve this problem, the surface geostrophic current for the equatorial band can be estimated by using the proposed method in the study of Lagerloef et al. (1999).

For calculating U_g , Equation (6) has been used. This component refers to the geostrophic current (Lagerloef et al., 1999).

$$ifU_g = -gZ \quad (6)$$

where U_g and Z are $u_g + iv_g$ and $\frac{\partial ADT}{\partial y} + i\frac{\partial ADT}{\partial x}$ respectively. The geostrophic velocity (U_β) with the approximation of the β plane ($f = \beta \cdot y$) using the derivative of Equation (7) can be calculated as follows (Lagerloef et al. 1999):

$$\beta U_\beta + \beta y \frac{\partial U_\beta}{\partial y} = ig \frac{\partial Z}{\partial y} \quad (7)$$

where $U_\beta = u_\beta + iv_\beta$ is in the equatorial band (U_β is related to the tropical region). In order to simplify the problem, Equation (7) can be changed into Equation (8) using the approximation of polynomial expansion:

$$\begin{aligned} Z_\beta &= Z_0 + Z_1\varphi + Z_2\varphi^2 + Z_3\varphi^3 \\ U_\beta &= \frac{ig}{\beta L}(Z_1 + Z_2\varphi + Z_3\varphi^2) \end{aligned} \quad (8)$$

Where L represents 1° in the equator (approximately equals to 111 km). Using Equation (5) as well as weighted functions of U_s and U_β , the surface geostrophic current between the equator and high latitudes can be reflected in Equation (9) (Lagerloef et al. 1999):

$$(u_g, v_g) = \omega_\beta(u_\beta, v_\beta) + \omega_s(u_s, v_s) \quad (9)$$

where ω_β and ω_s values in the equator are 1 and 0 respectively. If $\omega_\beta \rightarrow 0$ and $\omega_s \rightarrow 1$ in high latitudes, weighted functions can be considered as Equation (10).

$$\begin{aligned} \omega_\beta &= \exp\left[-(\varphi/\varphi_c)^2\right] \\ \omega_s &= 1 - \omega_\beta \end{aligned} \quad (10)$$

where φ_c is the longitudinal scale depending on the latitude and for the weight distribution in Equation (6), the value of 2.2° was chosen

for φ_c .

Eventually, the value of geostrophic current is calculated through Equation (11):

$$G = \sqrt{u_g^2 + v_g^2} \frac{m}{s} \quad (11)$$

3-2. The Wind Stress and The Ekman Surface Current

The Ekman surface current depends on the wind stress on the sea surface. The wind stress actually is the horizontal force of wind on the sea surface. Hence, the momentum transfer is carried out from the atmosphere to the ocean by the wind stress. The wind stress, T , can be calculated using Equation (12) (Stewart, 2009).

$$T = \rho_a C_D U_{10}^2 \quad (12)$$

where ρ_a is the air density which equals to 1.3 kg/m^3 , U_{10} is the wind speed at the height of 10 meters above the sea surface and C_D is the drag coefficient related to the 10-meter height (In such a way that the desired output is defined in accordance with this height). This coefficient depends on the wind speed. In order to attain the drag coefficient, several equations were proposed as follows, by Yelland and Taylor (1996) and Yelland et al. (1998):

$$\begin{aligned} 1000C_D &= 0.29 + \frac{3.1}{U_{10}} + \frac{7.7}{U_{10}^2} \quad (3 \leq U_{10} \leq 6 \text{ m/s}) \\ 1000C_D &= 0.60 + 0.071U_{10} \quad (6 \leq U_{10} \leq 26 \text{ m/s}) \end{aligned} \quad (13)$$

The value and the direction of the wind stress in January 2014 in Figure 5, are presented by Equation (12).

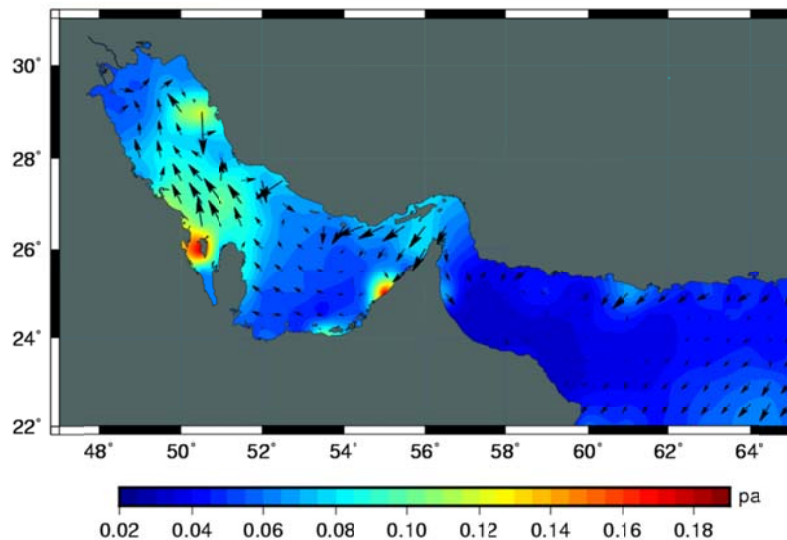


Figure 5. The value and direction of the wind stress (Pa) in January 2014.

The water movement induced by the wind drift is expressed by Ekman theory (theories which can be used in the ocean circulation). Being aware of dynamic effects of the bed friction on the water current and the surrounding environment, it is necessary to recognize features of the boundary layer, dubbed "Ekman layer". The Ekman layer is a layer located between the geostrophic current and the solid boundary, and the friction effect is so critical at this layer. This layer is formed in the lower part of the atmosphere and the seabed (Apel, 1990). In addition to Ekman layer in the seabed, another Ekman layer also exists on the sea surface which is due to the surface wind stress and is formed in the upper part of the seawater. Indeed, constant wind on the sea surface results in a horizontal boundary layer. This thin layer is the Ekman layer. Ekman (1905) suggested that under certain conditions (stable conditions), an equilibrium exists among the wind uniform stress, the Coriolis force, and the friction in the surface layer (Nitta and Yamada, 1989).

The velocity of the Ekman surface current ($U_e = u_e + iv_e$) in orbital or eastward component terms u_e , and meridional or northward component v_e , along the east direction (x) and north direction (y), directly conforms to Ekman equations for the equilibrium between the friction force and the Coriolis force, in the form of Equation (14) (Apel, 1990).

$$\begin{aligned} f v_e + \frac{1}{\rho} \frac{\partial T_{xz}}{\partial z} &= 0 \\ f u_e - \frac{1}{\rho} \frac{\partial T_{yz}}{\partial z} &= 0 \end{aligned} \quad (14)$$

Where f is the Coriolis parameter and equals to $2\Omega \sin \varphi$. The solution of Equation (14) can be considered as follows (Apel, 1990):

$$\begin{aligned} -f D_E v_e &= -\gamma u_e + \frac{1}{\rho} T_{xz} \\ f D_E u_e &= -\gamma v_e + \frac{1}{\rho} T_{yz} \end{aligned} \quad (15)$$

where γ is a linear drag coefficient that shows vertical viscosity terms as the body force on Ekman components; u_e and v_e are components of Ekman surface velocity in directions of x and y respectively; T_{xz} and T_{yz} are components of the stress

components of the wind in the directions x and y; ρ is the seawater density equal to 1025 kg/m^3 and D_E is the Ekman layer depth. The Ekman layer depth is considered as the effective depth of the wind drift current and is expressed by Equation (16).

$$D_E = \frac{7.6}{\sqrt{|\sin \varphi|}} U_{10} \quad (16)$$

Where φ is the latitude and U_{10} is the wind speed at a height of 10 meters above the sea surface. By the increase the Ekman layer depth, the current deviation occurs due to the Coriolis force. Ekman surface currents deviate 45° to the right and left direction of the wind on the surface, in the northern and southern hemisphere, respectively (Stewart, 2009).

U_e refers to the Ekman current component and can be calculated by Equation (17):

$$(if D_E + \gamma) U_e = T \quad (17)$$

Where $U_e = u_e + iv_e$ and $T = (T_{xz} + iT_{yz})/\rho$, T is the kinematic stress which has been calculated by considering $\rho = 1025 \text{ kg/m}^3$. In order to calculate the Ekman velocity, U_e , Equation (18) can be used (Stewart, 2009).

$$U_e = a_1 T \quad (18)$$

Equation (18) can be rewritten in the form of Equation (19).

$$a_1 = \frac{1}{if D_E + \gamma} = \frac{\gamma - if D_E}{\gamma^2 + f^2 D_E^2} \quad (19)$$

Where coefficient of a_1 is the reverse velocity dimension and refers to the scale of the kinematic wind stress, and a_1/ρ with the dimension of $\text{ms}^{-1}\text{Pa}^{-1}$ refers to the scale and dynamic wind stress. The real and the imaginary terms represent velocity components which are parallel and perpendicular to the wind stress respectively. When $f \rightarrow 0$, the imaginary term would be zero and the real term tends to $(a_1) \rightarrow 1/\gamma$, in this situation, the equatorial Ekman current depends on the lower part of the wind and the amplitude relative to the wind stress is determined by the reverse of the drag coefficient. The coefficient of a_1 is experimentally estimated according to Equation (18) using multiple linear

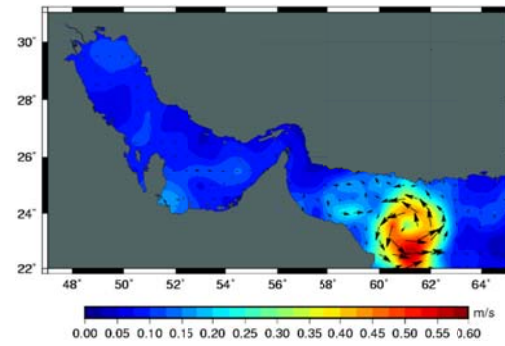
regression. Mixed linear regression creates real and imaginary parts for the coefficient of a_1 , in which the real term represents the longitudinal gradient along the wind direction and the imaginary term represents the cross gradient in the normal direction relative to the wind direction. Finally, in order to calculate the value of the Ekman current, Equation (20) is used:

$$G = \sqrt{u_e^2 + v_e^2} \frac{m}{s} \quad (20)$$

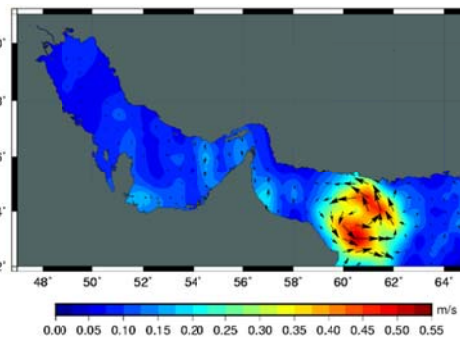
4. Results and Discussion and Conclusion

According to the presented explanations in the section 3, the absolute dynamic topography and the wind stress are used to calculate components of Ekman and geostrophic surface velocities respectively. Absolute dynamic topography and the wind stress can be achieved using Equations (4) and (12) respectively and a regular altitude

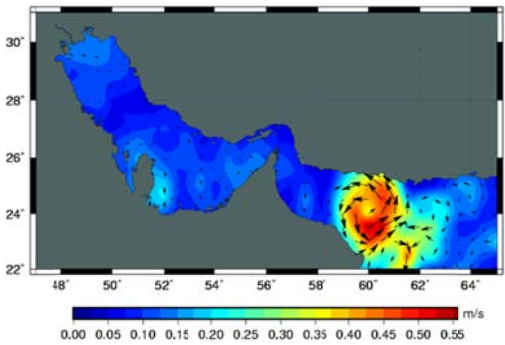
grid is then formed in order to calculate the absolute dynamic topography by interpolating SSH data. In the next step, the value and direction of geostrophic and Ekman currents are measured using Equations (9) and (11) as well as Equations (17) and (19) respectively, in forms of monthly data. These equations include some information about the current only in grid points and provide no information among the mentioned grid points. Grid dimension for solving equations is $5^\circ \times 5^\circ$. Ekman and geostrophic currents are calculated for grid points and finally, components of velocity were obtained for the currents. The value and direction of the geostrophic current as well as the Ekman current, in monthly time periods for 2014 in the region of the Persian Gulf and the Oman Sea are presented in Figures 6-1 to 6-12 and 7-1 to 7-12, respectively.



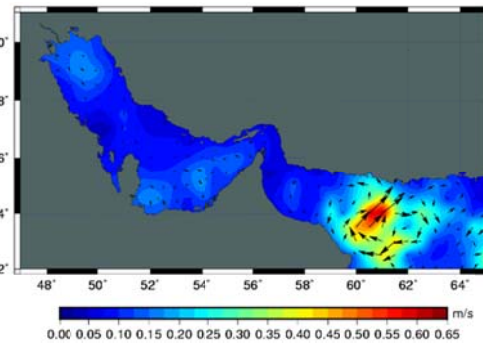
6-1. Jan 2014



6-2. Feb 2014



6-3. Mar 2014



6-4. Apr 2014

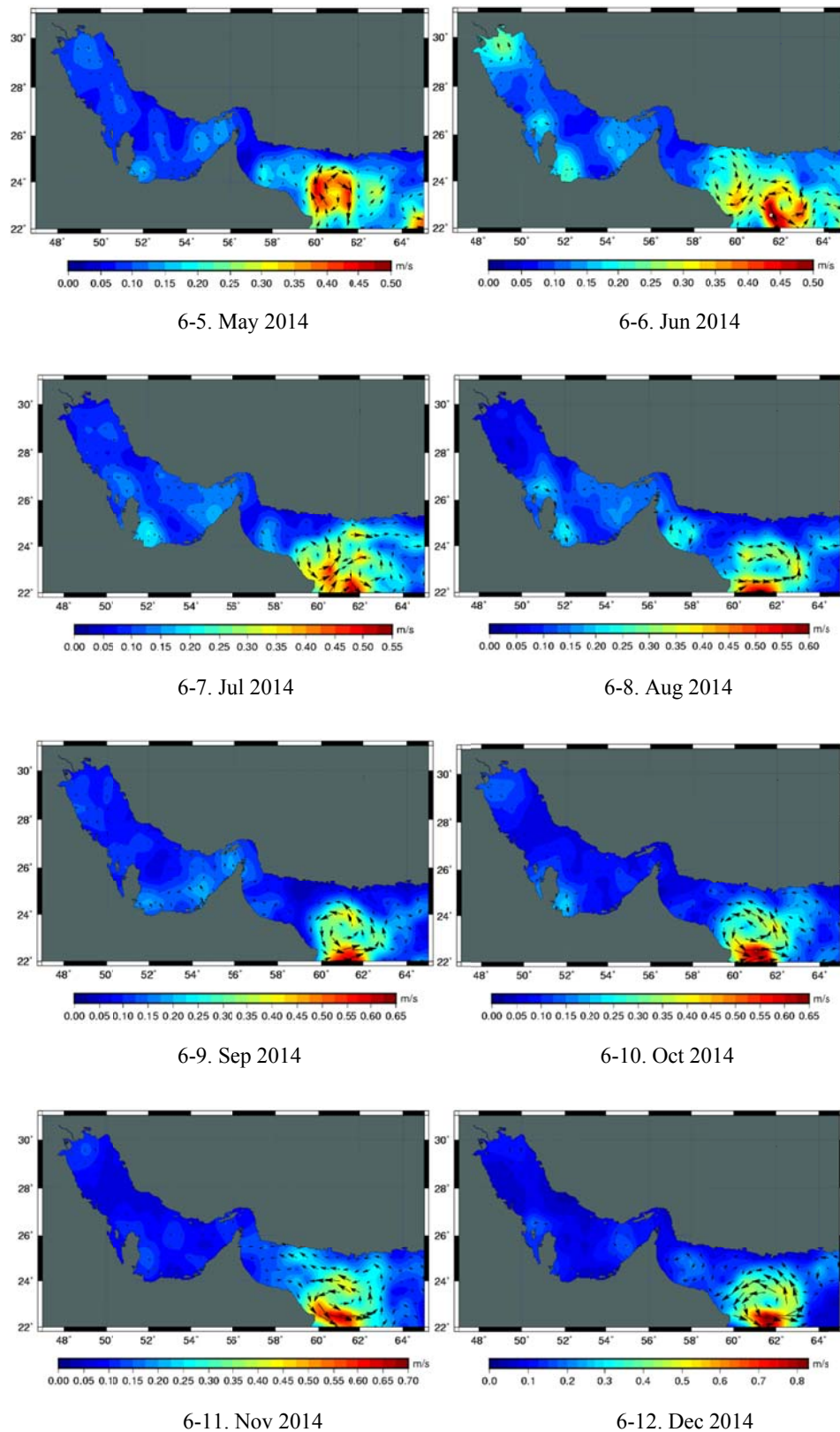
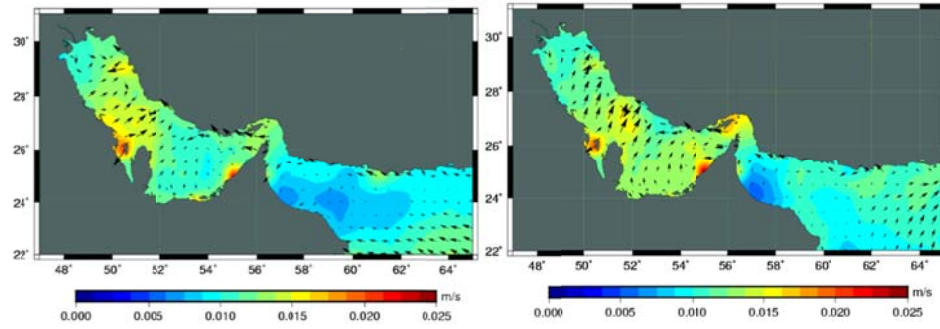
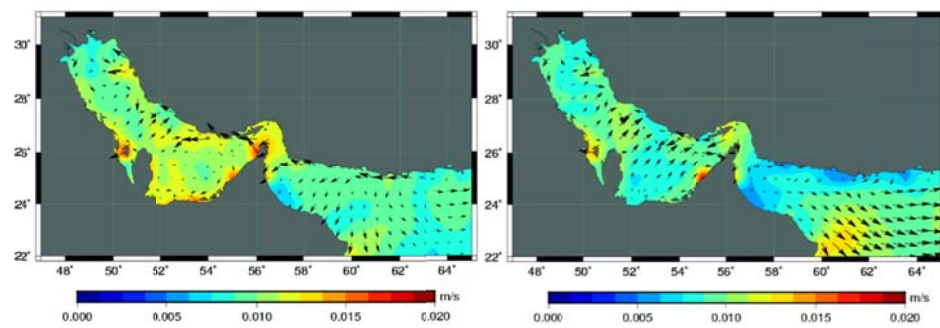


Figure 6. Figures 6-1 to 6-12 show the values and directions of geostrophic currents (m/s) using the absolute dynamic topography of Saral and Jason-2 satellites data in the year 2014.



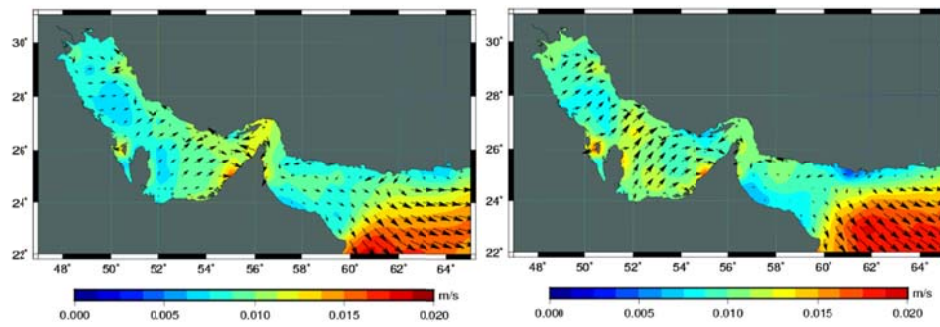
7-1. Jan 2014

7-2. Feb 2014



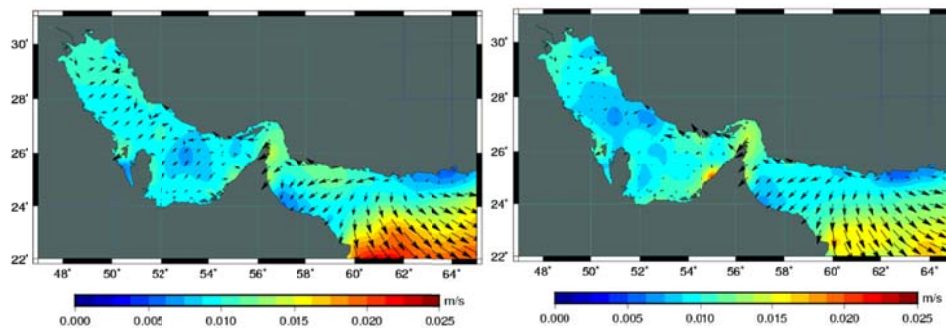
7-3. Mar 2014

7-4. Apr 2014



7-5. May 2014

7-6. Jun 2014



7-7. Jul 2014

7-8. Aug 2014

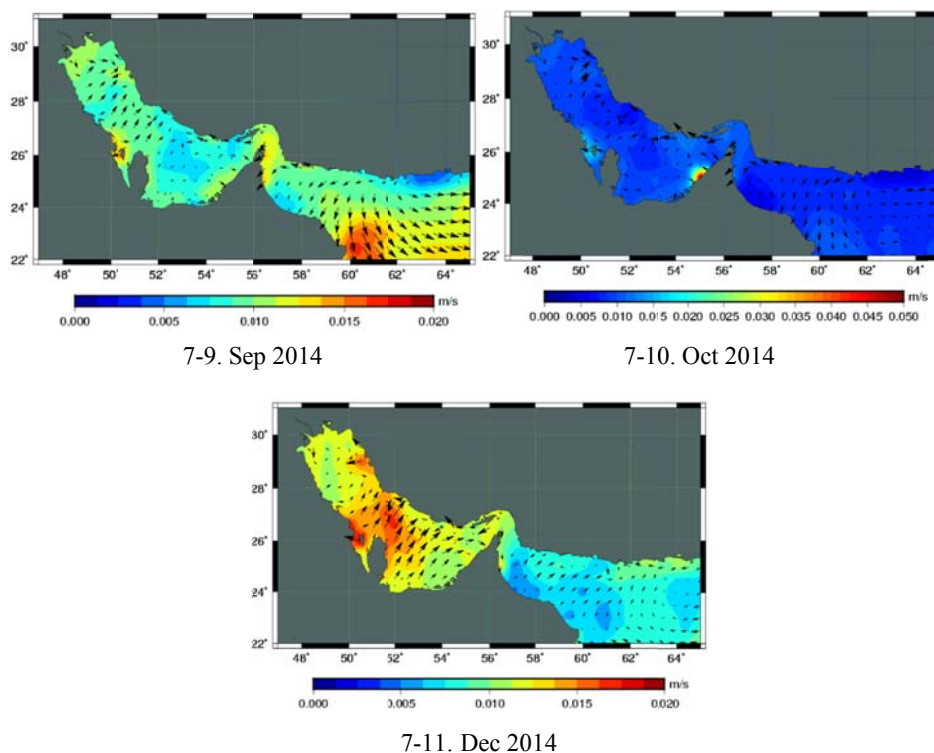


Figure 7. Figures 7-1 to 7-11 show the values and directions of the Ekman currents (m/s) using surface wind stress of ASCAT satellites data in the year 2014.

In Figures 6-1 to 6-12, vectors and the background color show the directions and values of surface geostrophic currents in the region of the Persian Gulf and the Oman Sea respectively. The existence of eddies is obvious in the region of the Persian Gulf and the Oman Sea indicating the existence of clockwise and anti-clockwise circulations. In inner parts of the Oman Sea, especially Jusk area and the Oman, the directions of currents have different forms and in spite of conforming to the major pattern, they have local circulations. In this part of the Oman Sea, a complicated current with two contradictory eddies exists. In the west side of the Oman Sea, there exists an eddy compatible with the clockwise movement and in the east side an eddy with an anti-clockwise movement exists. In regions between these two contradictory gyres, upwelling currents occur alongside the coasts of Iran. The circulation pattern in the region of Persian Gulf is anti-clockwise. In Strait of Hormuz, this circulation is originated from coasts of Iran and mostly from the surface, and near the coasts of Arabian countries,

this circulation exits from the inner part of the Persian Gulf (Reynolds, 1993; Swift and Bower, 2003). As can be seen in Figure 6, the direction of geostrophic movement is toward the southern coasts of the Persian Gulf, which is identical with the direction of the main circulation of the Persian Gulf. Therefore, geostrophic currents play a vital role in creating the main currents of the Persian Gulf. According to Figure 6, in the whole area have various velocities. Components of the velocity in the southern part of the Oman Sea are larger than components related to other parts of the Oman Sea and in the Persian Gulf. The observed geostrophic current average velocity changes in different months of the year. The average values of the velocity for 2014 ranges between 0.1391 m/s and 0.1673 m/s in different regions.

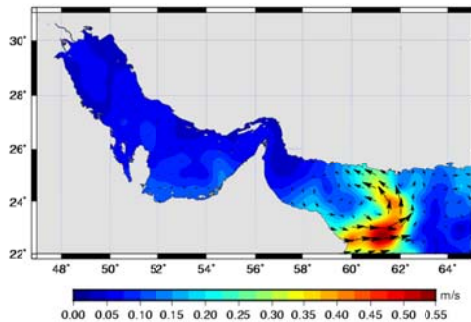
Figures 7-1 to 7-12 show the direction (as vectors) and values (as background color) of Ekman surface currents in the region of Persian Gulf and the Oman Sea in forms of monthly data for 2014. The observed Ekman velocity average changes in different months

of the year. The average values of the Ekman current range between 0.0092 m/s and 0.0117 m/s with the angle of 45° relative to the wind direction in various regions. The Ekman current can intensify some physical phenomena such as upwelling and downwelling which thereby can lead to certain effects on the environment, fisheries and fishing in small scales (Vignudelli et al., 2011). The direction of the Ekman surface currents in the regions of the Persian Gulf and the Oman Sea are different everywhere and depends completely on the wind direction. This direction is toward the sea when the westerly wind is blowing and upwelling currents is formed as a result, and when the easterly wind is blowing, the Ekman surface current direction is toward the coast and at that region, downwelling currents is created. In the northern region of the Persian Gulf and northwestern region of the Oman Sea, the Ekman current gives rise to the creation of upwelling currents and

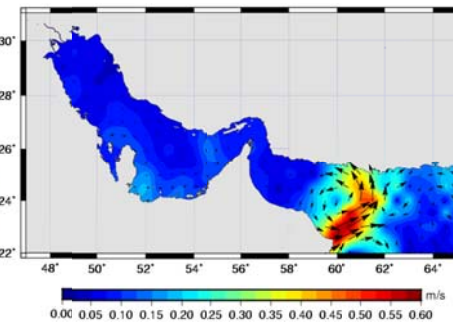
consequently, cold waters of the lower layer are brought to the sea surface. This phenomenon leads to the change of the surface water temperature. The risen water benefits from nutritious materials and its temperature is relatively lower than the surface water. Consequently, the food pyramid is boosted and as a result, the population of aquatic animals, especially fishes, increases.

4.2. Comparison with Local Measurements

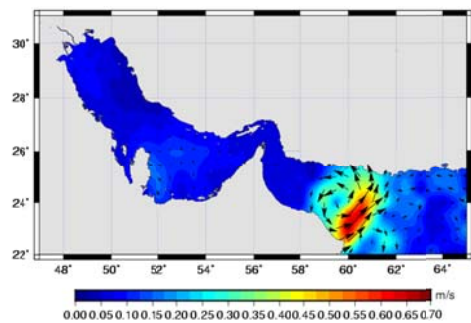
In order to check the accuracy and reliability of obtained results of geostrophic current values as well as Ekman current values by using altimetry satellite data and the surface wind data respectively, geostrophic current data presented by AVISO and Ekman current data reported by <http://coastwatch.pifsc.noaa.gov>, were used. The obtained results of this investigation in the year 2014 are depicted in Figures of 8-1 to 8-12 and 9-1 to 9-12.



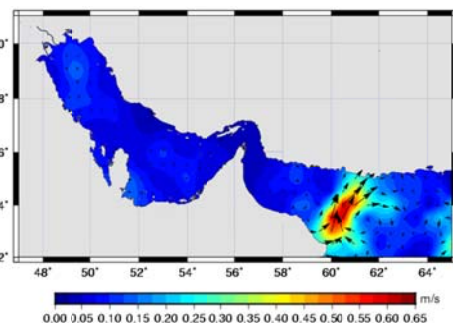
8-1. Jan 2014



8-2. Feb 2014



8-3. Mar 2014



8-4. Apr 2014

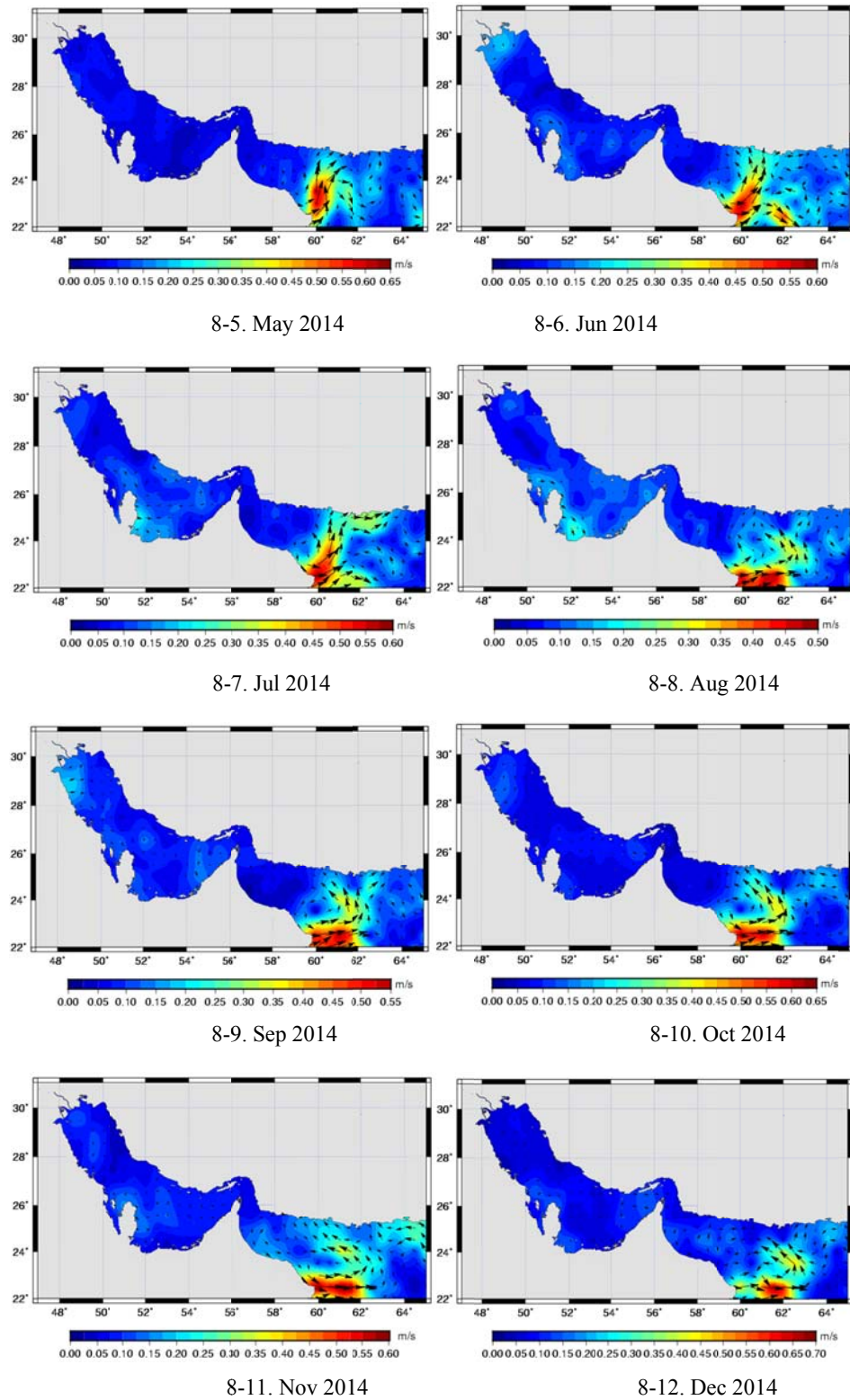
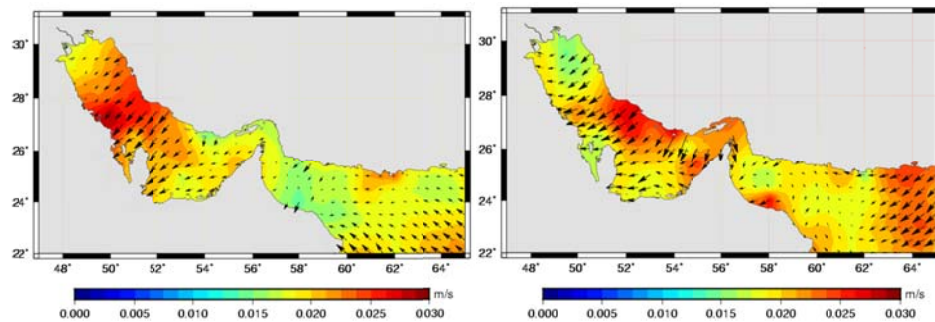
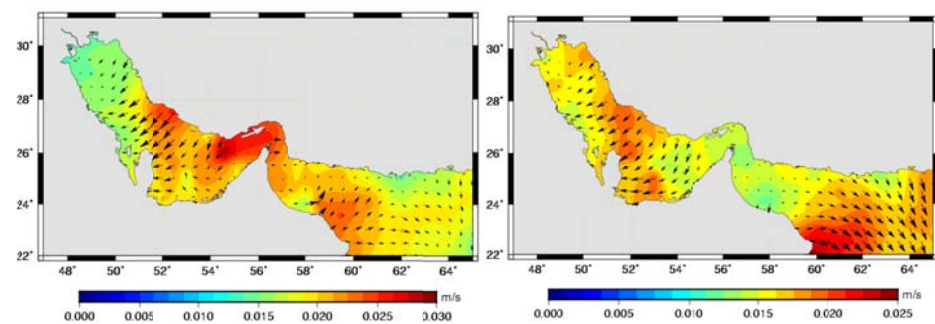


Figure 8. Figures 8-1 to 8-12 show the values and directions of the calculated geostrophic currents (m/s) by AVISO in the year 2014.



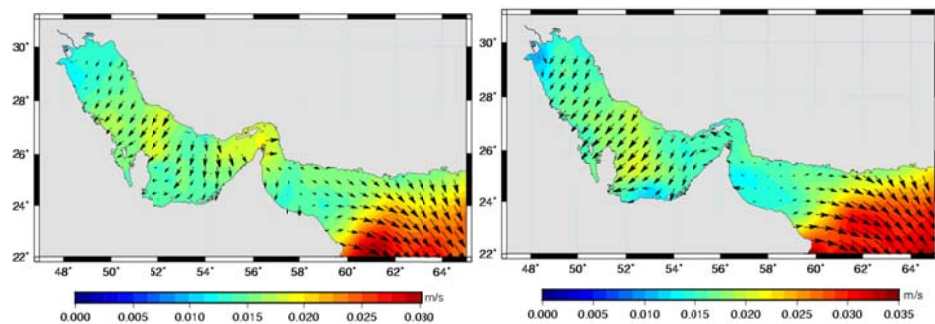
9-1. Jan 2014

9-2. Feb 2014



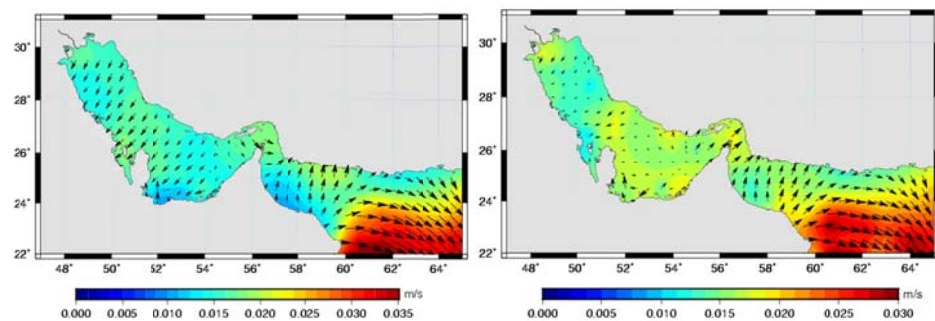
9-3. Mar 2014

9-4. Apr 2014



9-5. May 2014

9-6. Jun 2014



9-7. Jul 2014

9-8. Aug 2014

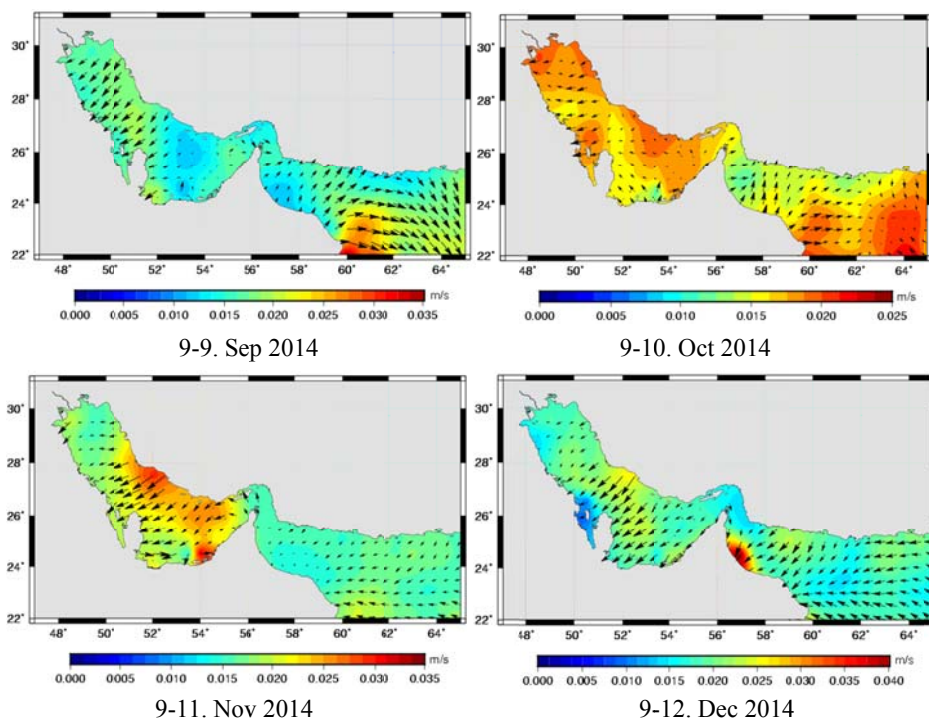


Figure 9. Figures 9-1 to 9-12 show the values and directions of the calculated Ekman currents (m/s) by NOAA in the year 2014.

Vectors in Figures 8-1 to 8-12 and 9-1 to 9-12 indicate the direction of surface geostrophic currents and Ekman surface currents respectively, and the background color in all figures shows the value of currents in both the Persian Gulf and the Oman Sea in monthly time periods for 2014. By comparing Figures 6 and 7 with 8 and 9, it can be concluded that Ekman and geostrophic equations can almost depict Ekman and geostrophic currents in the region of the Persian Gulf and the Oman Sea. Finally, obtained results of the geostrophic current calculated by altimetry data were

compared with the calculated geostrophic current through AVISO. In addition, results of the calculated Ekman current extracted from the data of the surface wind were also compared with the calculated Ekman current by NOAA. Results of this comparison are presented in Table 1 and 2. The difference between the calculated geostrophic current in this work and the calculated value by AVISO is 1 cm/s. For the Ekman current, this difference also equals to 1 cm/s. Hence, it can be inferred that the accuracy and reliability of obtained results are almost acceptable.

Table 1. Comparison of the results of the calculated geostrophic currents by altimetry data with the calculated geostrophic currents by AVISO.

Months Names	Calculated Geostrophic Current Using Altimetry Data (m/s)	Calculated Geostrophic Current Through AVISO (m/s)	Difference (m/s)
January	0.1407	0.1271	0.0136
February	0.1391	0.1435	0.0044
March	0.1601	0.1401	0.0200
April	0.1521	0.1234	0.0287
May	0.1405	0.1268	0.0137
June	0.1659	0.1461	0.0198
July	0.1575	0.1462	0.0113
August	0.1509	0.1278	0.0231
September	0.1472	0.1322	0.015
October	0.1464	0.1357	0.0107
November	0.1638	0.1468	0.017
December	0.1673	0.1366	0.0307

Table 2. Comparison results of the calculated Ekman currents by data of the surface wind with the calculated Ekman currents by NOAA.

Months Names	Calculated Ekman Current By Data of the Surface Wind (m/s)	Calculated Ekman Current by NOAA(m/s)	Difference (m/s)
January	0.0109	0.0196	0.0087
February	0.0114	0.0204	0.009
March	0.0100	0.0194	0.0094
April	0.0092	0.0168	0.0076
May	0.0104	0.0178	0.0074
June	0.0117	0.0202	0.0085
July	0.0115	0.0190	0.0075
August	0.0108	0.0181	0.0073
September	0.0100	0.0173	0.0073
October	0.0092	0.0170	0.0078
November	0.0099	0.0191	0.0092

5. Conclusion

In the current study, in order to investigate the surface geostrophic current, SSH data of both altimetry satellites of Saral and Jason-2 as well as geoid data of EGM08 model were used. To examine Ekman surface currents, surface wind data from the ASCAT satellites were used. For both currents, data were extracted in forms of monthly data, for 2014. The studied area was the region of the Persian Gulf and the Oman Sea. In order to calculate surface geostrophic currents, the motion of was used considering changes of the Coriolis index with latitude and the pressure gradient. Additionally, the approximation of a beta plane, as well as hydrostatic and stable aspects of the current were also used. In these equations, frictional terms are not taken into account. These equations are known as geostrophic equations obtained by the balance between the Coriolis force and the friction force.

In the surface layer of the Persian Gulf and the Oman Sea, eddies are formed indicating the compatible clockwise or anti-clockwise circulation of water evidently. In inner parts of the Oman Sea, especially the region of Jusk and Oman, a complicated current with two opposed circulations exists. In regions between these two cycles which are along the coast of Iran, upwelling currents occur. The dominant direction in geostrophic currents is toward the southern coastal region of the Persian Gulf, which is along the direction of the main current of the Persian Gulf. Hence, geostrophic currents can play a determining

role as the mains component of the Persian Gulf. The average values of geostrophic currents reach maximum value in December, while its nadir is in February.

For calculating the Ekman current, an equation was used by considering changes of the Coriolis index with the latitude and friction effects assuming that the currents are steady. For solving these equations, the Ekman theory was used. These equations are known as Ekman equations, which are attained from the equilibrium between the Coriolis force and the friction force. Based on the Ekman theory, surface currents due to the wind, deviate 45° along the right and the left direction of the wind, in the northern and southern hemispheres respectively. In other words, when the westerly wind blows, the wind direction is toward the sea and intensifies the formation of upwelling currents, and when the easterly wind blows, the wind direction is toward the coast and it culminates in the creation of down welling currents.

In the northern regions of the Persian Gulf and northwestern regions of the Oman Sea, the Ekman current leads to the creation of upwelling making cold waters of the lower layer move to the surface of the sea. The result of this phenomenon is change of water surface temperature. Hence the risen water enriched with nutritious materials and also benefits from a lower temperature. Therefore, the food pyramid is reinforced and the population of aquatic animals noticeably increases. Average values of Ekman currents

are maximum and minimum in June and October respectively. Results obtained from altimetry satellite data and satellites surface wind data are used in the calculation of geostrophic and Ekman surface currents respectively with a satisfactory compatibility with calculated data by AVISO and NOAA. The different values for both currents values were obtained as 1 cm/s for 2014, which confirms the accuracy and correctness of obtained currents. Considering Ekman and geostrophic currents in intended time periods, the dynamics of sea surface currents can be realized and then be analyzed.

References

- Andersen, B., 2010, Satellite derived reference surfaces for surveying. Dtu-Space. Copenhagen. Denmark.
- Aken, H. M. van, 2007, The Oceanic Thermohaline Circulation: An Introduction. Springer Science & Business Media.
- Apel, J. R., 1990, Principle, of Ocean Physics. Academic Press, chp. 6.
- AVISO, 2012, DT CorSSH and DT SLA Product Handbook - Aviso. France.
- Bowditch, N., 2012, The American Practical Navigator. CreateSpace Independent Publishing Platform.
- Dawe, J. T. and Thompson, L., 2006, Effect of ocean surface currents on wind stress, heat flux, and wind power input to the ocean. *Geophys. Res. Lett.*, 33, L09604. doi:10.1029/2006GL025784.
- Deng, X., Griffin, D. A., Ridgway, K., Church, J. A., Featherstone, W. E., White, N. J. and Cahill, M., 2011, Satellite Altimetry for Geodetic, Oceanographic, and Climate Studies in the Australian Region. In: Vignudelli, S., Kostianoy, A.G., Cipollini, P., Benveniste, J. (Eds.), *Coastal Altimetry*. Springer Berlin Heidelberg, 473–508.
- Ekman, V. W., 1905, On the influence of the Earth's rotation on ocean currents. *Arkiv for Matematik, Astronomi, och Fysik*, 2(11).
- Fleet, D. J. and Weiss, Y., 2005, Optical Flow Estimation. <http://coastwatch.pifsc.noaa.gov>. <http://oceanwatch.pifsc.noaa.gov>.
- Forman, M. G. G., 1998, Manual for tidal currents analysis and prediction, pacific marine science report. Podaac and Podaac Merged Gdr (Topex/Poseidon) Users Handbook. Jpl, D-11007, November.
- Stewart, R. H. 2008, Introduction to physical oceanography, Department of Oceanography, Texas A & M University.
- Lagerloef, G. S. E., Mitchum, G. T., Lukas, R. B. and Niiler, P. P., 1999, Tropical Pacific near-surface currents estimated from altimeter, wind, and drifter data. *J. Geophys. Res.*, 104(C10), 23, 313–23, 326, doi:10.1029/1999JC900197.
- Munk, W. H., 1950, On the wind-driven ocean circulation. *J. Meteorology*, 7(2), 79–93.
- Nansen, F. and Sverdrup, O. N., 1898, Farthest north: being a record of a voyage of exploration of the ship "Fram" 1893-96, and of a fifteen month's sleigh journey by Dr. Nansen and Lieut. Johannsen (Vol. 1). Harper & brothers.
- Nitta, T. and Yamada, S., 1989, Recent warming of tropical sea surface temperature and its relationship to the Northern Hemisphere circulation. *Journal of the Meteorological Society of Japan*. Ser. II, 67(3), pp.375-383.
- Reynolds, R. M., 1993, Physical Oceanography of the Gulf, Strait of Hormuz, and the Gulf of Oman--Results from the Mt Mitchell Expedition. *Marine Pollution Bulletin*, 27, 35-59, Printed in Great Britain.
- Parvazi, K., Asgari, J., Amirismkooei, A. R., and Tajfirooz, B., 2015, Determination of difference between datum and reference ellipsoid by using of analysis of altimetry data of Topex/Poseidon, Jason-1 and observations of coastal tide gauges, 5(1).
- Picot, N., Case, K., Desai, S. and Vincent, P., 2003. AVISO and PODAAC user handbook. IGDR and. <http://www.aviso>.
- Reynolds, R. W. and Smith, T. M., 1994, Improved global sea surface temperature analyses using optimum interpolation. *J. Clim.*, 7, 929–948. doi:10.1175/1520-0442(1994)007<0929:IGSSTA>2.0.CO;2
- Scharffenberg, M. G. and Stammer, D., 2010, Seasonal variations of the large-scale geostrophic flow field and eddy kinetic energy inferred from the TOPEX/Poseidon and Jason-1 tandem mission data, *J. Geophys. Res.*, 115, C02008, doi:10.1029/2008JC005242.1.

- Shum, C. K. and Braun, A., 2004, Satellite Altimetry and Gravimetry. Lecture notes presented at Norwegian University of Science and Technology (NTNU), Trondheim, Norway, <http://www.octas.statkart>.
- Stewart, R. H., 2009, Introduction to Physical Oceanography. Orange Grove Texts Plus, College Station, Tex.
- Stommel, H., 1948, The westward intensification of wind-driven ocean currents. Transactions, American Geophysical Union, 29(2), 202–206.
- Sverdrup, H. U., 1947, Wind-driven currents in a baroclinic ocean: with application to the equatorial currents of the eastern Pacific. Proceedings of the National Academy of Sciences, 33(11), 318–326.
- Swift, S. A. and Bower, A. S., 2003, Formation and circulation of dense water in the Persian/Arabian Gulf. J. Geophys. Res., 108(C1), 3004, doi:10.1029/2002JC001360.
- Vignudelli, S., Kostianoy, A., Cipollini, P., and Benveniste, J., 2011, Coastal Altimetry, Springer, German, Berlin.
- Yelland, M. and Taylor, P. K., 1996, Wind stress measurements from the open ocean. J. Physical Oceanography, 26(4), 541–558.
- Yelland, M. J., Moat, B. I. Taylor, P. K. Pascal, R. W. Hutchings, J. and Cornell, V. C., 1998, Wind stress measurements from the open ocean corrected for airflow distortion by the ship. Journal of Physical Oceanography, 28(7), 1511–1526.
- Zonn, S., Kosarev, A. N., Glantz, M. and Kostianoy, A. G., 2010, The Caspian Sea Encyclopedia, 2010 edition. ed. Springer, Berlin; London.